Non-Markovian response of ultrafast coherent electronic ring currents in chiral aromatic molecules in a condensed phase

H. Mineo, S. H. Lin, Y. Fujimura, J. Xu, R. X. Xu, and Y. J. Yan

---

Articles you may be interested in

Non-Markovian stochastic Schrödinger equation at finite temperatures for charge carrier dynamics in organic crystals
J. Chem. Phys. **138**, 014111 (2013); 10.1063/1.4773319

Ultrafast electron thermalization in a magnetic layered Au/Co/Au film
J. Appl. Phys. **104**, 094301 (2008); 10.1063/1.3005986

Ultrafast nonradiative dynamics in electronically excited hexafluorobenzene by femtosecond time-resolved mass spectrometry
J. Chem. Phys. **128**, 164314 (2008); 10.1063/1.2907859

Chemistry, photophysics, and ultrafast kinetics of two structurally related Schiff bases containing the naphthalene or quinoline ring
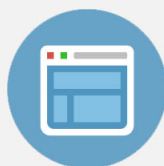J. Chem. Phys. **125**, 184508 (2006); 10.1063/1.2371058

Spectroscopy and ultrafast dynamics of the 2A 1 state of Z-hexatriene in gas phase
J. Chem. Phys. **106**, 2205 (1997); 10.1063/1.474080

Non-Markovian response of ultrafast coherent electronic ring currents in chiral aromatic molecules in a condensed phase

H. Mineo,[1] S. H. Lin,[1,2] Y. Fujimura,[1,3] J. Xu,[4,5] R. X. Xu,[6] and Y. J. Yan[5,6]

[1]*Institute of Atomic and Molecular Sciences, Academia Sinica, Taipei 10617, Taiwan*
[2]*Department of Applied Chemistry, Institute of Molecular Science and Center for Interdisciplinary Molecular Science, National Chiao-Tung University, Hsin-Chu 300, Taiwan*
[3]*Department of Chemistry, Graduate School of Science, Tohoku University, Sendai 980-8578, Japan*
[4]*Department of Chemistry, Nankai University, Tianjin 300071, China*
[5]*Department of Chemistry, Hong Kong University of Science and Technology, Kowloon, Hong Kong*
[6]*Hefei National Laboratory for Physical Sciences at the Microscale, University of Science and Technology of China, Hefei, Anhui 230026, China*

Results of a theoretical study on non-Markov response for femtosecond laser-driven coherent ring currents in chiral aromatic molecules embedded in a condensed phase are presented. Coherent ring currents are generated by coherent excitation of a pair of quasi-degenerated π-electronic excited states. The coherent electronic dynamical behaviors are strongly influenced by interactions between the electronic system and phonon bath in a condensed phase. Here, the bath correlation time is not instantaneous but should be taken to be a finite time in ultrashort time-resolved experiments. In such a case, Markov approximation breaks down. A hierarchical master equation approach for an improved semiclassical Drude dissipation model was adopted to examine the non-Markov effects on ultrafast coherent electronic ring currents of (P)-2,2′-biphenol in a condensed phase. Time evolution of the coherent ring current derived in the hierarchical master equation approach was calculated and compared with those in the Drude model in the Markov approximation and in the static limit. The results show how non-Markovian behaviors in quantum beat signals of ring currents depend on the Drude bath damping constant. Effects of temperatures on ultrafast coherent electronic ring currents are also clarified. © *2013 AIP Publishing LLC*. [http://dx.doi.org/10.1063/1.4834035]

I. INTRODUCTION

In recent years, laser control of currents in molecular systems and solids has attracted much attention for realization of optoelectronic devices.[1–6] Quantum dynamical simulations for the creation of ultrafast ring currents in organic molecules by ultrashort UV laser pulses have been presented.[7–14] The π-electron ring current in Mg-porphyrin could be induced by a few cycles of circularly polarized UV laser pulses within a few femtoseconds.[8–10] In the process, circularly polarized light transfers photon angular momentum to degenerated electronically excited states of Mg-porphyrin. The use of linearly polarized UV laser pulses to create π-electron rotation along the ring of 2,5-dichloro[n](3,6) pyrazinophane was proposed by Kanno *et al.*[11–15] An efficient method for multi-dimensional quantum switching of π-electron rotation in (P)-2,2′-biphenol was developed by Mineo *et al.*[16,17] These are chiral molecules, with planar chirality and axial chirality, respectively. The aromatic rings in the study have no degenerate electronic states, but rather create transient electronic angular momenta. That is that the electronic angular momentum along each aromatic ring can be generated by coherent excitation of a pair of nondegenerate excited states. The created current in this case would be referred to as coherent ring current or quantum beats of ring currents. On the other hand, the ring current in Mg-porphyrin, created via optically active degenerate excited states, is essentially incoherent. As the characteristic features for the quantum electric

current and the classical one are concerned, coherent ring current corresponds to alternative current, while incoherent current corresponds to direct current.

In order to realize ultrafast switching devices of organic molecules, however, there remain many unsolved issues. One of the key issues is to clarify effects of environment on coherent ring current because devices consist of current-generating aromatic molecules which form a solid or are embedded in a condensed phase. In a previous study[17] we treated system-bath interaction effects on coherent ring currents within the Markov approximation, assuming that the interaction is instantaneous and there is no back action from the heat bath. The results showed that quantum beats (time-dependent behaviors) of coherent ring currents and the induced magnetic fields decrease with its exponential-decay envelope as time develops. It should be noted that coherent behaviors take place in an ultrashort time regime, within hundreds of femtoseconds, which is the same order of correlation time as that of the bath modes. For such a case, the Markov approximation may break down, and we have to explicitly take into account the back action of molecular system on heat bath.

In this paper, we clarify non-Markovian effects of environments on coherent ring currents in chiral aromatic molecules coupled with heat bath modes. For this purpose, we adopt the hierarchical equations of motion (HEOM) approach in an improved semiclassical Drude dissipation model.[18] The HEOM formalism employed here has been developed by Tanimura and co-workers[19–21] and Yan and co-workers[22–27]

mainly from the calculus on the Feynman-Vernon's influence functional path integral.[28] Shao and co-workers have also derived this formalism via a stochastic field description.[29–31] The HEOM formalism has been applied to many fields, such as electron transfer,[32,33] nonlinear optical spectroscopy,[34–37] and transient quantum transport.[38–40] Recently it is used as a standard theoretical tool for exploring the excitation energy transport processes in photosynthetic biological systems.[41–48] Non-Markovianicity or memory of noise causes also prominent features in quantum information such as the revival of entanglement after its "sudden death."[49,50] A dynamic measure for the degree of non-Markovian behavior in open quantum system had been also proposed with respect to a flow of information from the environment back to the system.[51,52]

This paper is organized as follows. In Sec. II, we briefly present a procedure for the HEOM approach in the semiclassical Drude dissipation model. In Sec. III, numerical simulation results of quantum beats of coherent ring currents of (P)-2-2′-biphenols in a condensed phase are presented and the effects of non-Markovian response on the ultrashort coherent behaviors are discussed. In Sec. IV, we summarize the present work.

II. HIERARCHICAL EQUATION OF MOTION (HEOM) APPROACH FOR COHERENT ELECTRIC RING CURRENTS OF CHIRAL MOLECULES IN A HEAT BATH

Consider a total system consisting of a chiral aromatic molecule in a heat bath. Laser pulses are applied to the system and are assumed to interact with the π-electronic states of the molecule but not with the bath mode. The π-electronic states are modulated by stochastic heat bath of the solvent. The interaction between the molecule and laser field is taken into account within the semi-classical theory.

Time-dependent coherent electron ring current, $I(t)$, is defined in terms of the expectation value of current density operator as

$$I(t) = \text{Tr}[\rho(t)\hat{I}], \qquad (1)$$

where $\rho(t)$ is the molecular density operator and $\hat{I}$, current density operator, is given as

$$\hat{I} = \frac{e\hbar}{2m_e i}(\vec{\nabla} - \overleftarrow{\nabla}). \qquad (2)$$

Here, $\vec{\nabla}(\overleftarrow{\nabla})$ denotes the nabra operating the atomic orbital on the right-hand (left-hand) side.

The Hamiltonian of the total system, H_T, is given in the semiclassical molecule–laser interaction as

$$H_T = H_M + H_B + F_{MR}(t) + F_{MB}(t), \qquad (3)$$

where H_M is the molecular system Hamiltonian, H_B is the bath Hamiltonian, $F_{MR}(t)$ is the molecular system-radiation interaction operator, and $F_{MB}(t)$ is the stochastic molecular system–bath interaction operator that can be generally expressed as $F_{MB}(t) = \sum_a Q_a (F_B(t))_a$. Here, the system operators $\{Q_a\}$ are called dissipative modes through which the stochastic bath operators $\{(F_B(t))_a\}$ acting on the system. In this work we choose $Q_a = |a\rangle\langle a|$ for the solvent bath

induced excited states $\{a\}$ energy fluctuation, with respective to the ground state. As only two electronic excited states will be considered in this work, we have $a = 1, 2$ in the following.

By tracing out the total composite system density operator over the bath variables, the reduced molecular system density operator, $\rho(t) \equiv \rho_0(t)$, can be described by the HEOM formalism, with the aid of a set of well-defined auxiliary density operators (ADOs), $\{\rho_n(t)\}$, as

$$\frac{\partial}{\partial t}\rho_n(t) = -(iL_s(t) + \delta R_n + \gamma_n)\rho_n(t) + \rho_n^{(-)}(t) + \rho_n^{(+)}(t). \qquad (4)$$

Here, $L_s(t) \, O \equiv [H_M + F_{MR}(t), O]$ defines the reduced system Liouvillian, $L_s(t)$, under the external classical driving fields, $\rho_n(t)$ is an nth-tier ADO, with the index n being a collection of indices, i.e., $n \equiv \{n_{11}, n_{12}, \ldots, n_{1N}, n_{21}, \ldots, n_{2N}\}$ and $\rho_n(t) = \rho_{n_{11},n_{12},\ldots,n_{2N}}(t)$ for $n = \sum_{a=1}^{2}\sum_{k=1}^{N} n_{ak}$ being the tier level. The reduced density matrix, $r(t) \equiv r_0(t)$, is the zeroth-tier ADO, and the Markov approximation can be obtained from Eq. (4) truncated at the tier level of $n = 1$ with setting $N = 0$. In Eq. (4), $\rho_n^{(\pm)}(t)$ describes how the given nth-tier ADO, $\rho_n(t)$, depends on its associated $(n \pm 1)$th-tier ADOs, and γ_n is a damping parameter which collects the underlying memory components, while δR_n is a super operator for a partial inclusion of the residue dissipation. The explicit expressions of these quantities are dictated by the exponential series expansion of bath correlation functions and will be specified as follows. The initial thermal equilibrium conditions before external field action can be obtained via the steady-state solution to HEOM. The resulted initial nonzero ADOs take account for the initial system-bath correlations at thermal equilibrium. In this work, the system before excitation is initially at the electronic ground state with the corresponding canonical thermal solvent environment.

In the stochastic bath model, the organization energy λ and damping parameter γ are parameters to specify the bath mode space. The Drude bath spectral density function is given as

$$J_a(\omega) = \frac{2\lambda_a \gamma_{a,D}\omega}{\omega^2 + \gamma_{a,D}^2}. \qquad (5)$$

This indicates that reorganization energy can be obtained by $\lambda_a = \int d\omega \frac{J_a(\omega)}{\pi\omega}$.

The Boson bath correlation function at temperature T is written through the fluctuation–dissipation theorem as

$$C_a(t) \equiv \langle F_{a,B}(t)F_{a,B}(0)\rangle_B$$
$$= \frac{1}{\pi}\int_{-\infty}^{\infty} d\omega \exp(-i\omega t)f(\beta\omega)J_a(\omega). \qquad (6)$$

Here, $f(\beta\omega)$ denotes the Bose-Einstein distribution function, $f(\beta\omega) = \frac{1}{1-\exp(-\beta\omega)}$ with $\beta = 1/(k_B T)$. The correlation function Eq. (6) can be expanded in the expansion series as

$$C_a(t) = \sum_{k=D,1}^{N} c_{a,k}\exp(-\gamma_{a,k}t) + \delta C_{a,N}(t). \qquad (7)$$

Here, $\gamma_{a,D}$ comes from the Drude spectral density function of Eq. (5), and $\gamma_{a,k} = \gamma_k$ with $k = 1, 2, \ldots, N$ comes from the poles of $f(\beta\omega)$ in $C(t)$. The exponential series expansion

of the correlation function can be evaluated using the standard contour integration technique.

Efficient HEOM algorithms have been developed by Yan's group.[18] They proposed an optimized HEOM theory, on the basis of an optimal family of Padé spectrum decomposition (PSD) schemes for Bose-Einstein distribution function,[25] and identified the [N/N] PSD is the best for Drude dissipation.[18, 26] The optimized HEOM theory, together with its simple criterion on accuracy control, have been demonstrated extensively, covering such as spin-Boson dynamics, coherent two-dimensional nonlinear spectroscopy, and dispersed transient absorption signals of a model dimer system at different temperatures.

In the [N/N] PSD scheme, the Bose function, $f(x)$ $\approx f_{[N/N]}(x)$, is exact up to $O((x)^{4N+1})$. It reads

$$\frac{1}{1-\exp(-x)} \approx f_{[N/N]}(x) + O(x^{4N+1})$$

$$= \frac{1}{x} + \frac{1}{2} + \sum_{k=1}^{N} \frac{2\eta_k x}{x^2 + \beta^2 \gamma_k^2} + R_N x + O(x^{4N+1}), \tag{8}$$

where $x = \beta\omega$, $R_N = \frac{1}{4(N+1)(2N+3)}$, and η_k and $\beta\gamma_k$ are PSD coefficients and poles that are all positive.[25] Using then the fluctuation-dissipation theorem, Eq. (6), the exponential series expansion of the Drude bath correlation function, Eq. (7), can be obtained via the contour integral on the lower half plane. We obtain

$$c_{a,D} = -2i\lambda_a\gamma_{a,D} f_{[N/N]}(\beta\omega)\big|_{\omega=-i\gamma_{a,D}}, \tag{9a}$$

$$c_{a,k} = \frac{2\eta_k}{i\beta} J_a(\omega)\big|_{\omega=-i\gamma_k} \quad (k=1,\ldots N), \tag{9b}$$

$$\delta C_{a,N}(t) \approx 2\Delta_{a,N}\delta(t), \tag{9c}$$

where $\Delta_{a,N} = 2\lambda_a\beta\gamma_{a,D}R_N$. The optimized HEOM formalism can then be obtained without further approximation. The only approximation is performed in the white noise treatment of the residue, $\delta C_N(t)$, by Eq. (9c). This results in the residue dissipation superoperator, δR_n in Eq. (4), a white noise form of

$$\delta R_n \rho_n(t) = \sum_a \Delta_{a,N} [Q_a, [Q_a, \rho_n(t)]]. \tag{10}$$

The damping parameter γ_n in Eq. (4) is given as

$$\gamma_n = \sum_a \sum_{k=D,1}^{N} n_{a,k}\gamma_k. \tag{11}$$

The tier-down and tier-up operators are, respectively, expressed as

$$\rho_n^{(-)}(t)$$
$$= -i\sum_a \sum_{k=D,1}^{N} \sqrt{\frac{n_{a,k}}{|c_{a,k}|}} \left(c_{a,k}Q_a\rho_{a,n_{a,k}^-}(t) - c_{a,k}^*\rho_{a,n_{a,k}^-}(t)Q_a\right) \tag{12}$$

and

$$\rho_n^{(+)}(t) = -i\sum_a \sum_{k=D,1}^{N} \sqrt{(n_{a,k}+1)|c_{a,k}|}[Q_a, \rho_{a,n_{a,k}^+}(t)]. \tag{13}$$

Here, $\rho_{a,n_{a,k}^-}(\rho_{a,n_{a,k}^+})$, with the indices $n_{a,k}^\pm \equiv \{n_{11}, \ldots, n_{a,k} \pm 1, \ldots, n_{2N}\}$, is the associated $(n-1)$th $((n+1)$th)-tier ADO.

III. RESULTS AND DISCUSSION

We present the results of application of the HEOM procedure to coherent ring currents for a real model system of (P)-2,2′-biphenol in a condensed phase. Quasi-degenerate electronic excited states (b_1 and b_2) of (P)-2,2′-biphenol were selected for simplicity. The two electronic states belong to the totally symmetric irreducible representation. The difference in energy between these excited states is 0.065 eV, which was calculated by using the TD-DFT B3LYP level of theory.[16,53] The two transition moments are along the short and long axes of (P)-2,2′-biphenols and are nearly orthogonal to each other. The electric field of the laser and pulse, $\boldsymbol{E}(t)$, was assumed to have the form $\boldsymbol{E}(t) = \boldsymbol{A}(t)\cos(\omega_L t)$, where $\boldsymbol{A}(t)$ is the amplitude of the pulse with a linearly polarized polarization vector and ω_L is the laser central frequency. For model simulations, a pulse excitation of (P)-2,2′-biphenol in the ground state was taken into account. The following laser pulse parameter set was used:

$$A(t) = F_0 g\left(t, t_i = 0, t_f = \frac{2\pi}{\omega_{b2b1}} = 10\,\text{fs}\right),$$

with $F_0 = 6.0$ GV/m, and

$$g(t, t_i, t_f) = \theta\left(t_i < t < t_f\right)\sin^2\left(\pi\frac{t-t_i}{t_f-t_i}\right).$$

Here, $\theta(t_i < t < t_f)$ is a step function; $\theta(t_i < t < t_f) = 1$ for $t_i < t < t_f$ and zero for other cases.

The direction of the linearly polarized pulse is taken to generate a coherent superposition of the two electronic states. The central frequency satisfies $\omega_L = (E_{b1} + E_{b2})/2$. Effects of inhomogeneous distribution of (P)-2,2′-biphenols were omitted for simplicity. An improved Drude model was adopted as the heat bath modes.

In this work, we assume that the bath influence on each electronic state can be described with the same spectral density function [cf. Eq. (5)]. It is noted that the reorganization energy, $\lambda = \lambda_1 + \lambda_2$ (where we assume $\lambda_1 = \lambda_2$) specifies the system-bath coupling strength. Two extreme cases can be considered: one is a weak system-bath coupling case, in which λ is small compared with the energy difference between quasi-degenerate two electronic states, ΔE, i.e., $\lambda < \Delta E$. In this case it should be noted that $\lambda < \Delta E$ if $\gamma_D > \Delta E$, which corresponds to the motional narrowing limit. The other is a strong coupling case in which $\lambda > \Delta E$, i.e., $\frac{1}{\Delta E} < \frac{1}{\lambda}$. The other parameter, the damping parameter, γ_D, which we assume $\gamma_{1,D} = \gamma_{2,D} = \gamma_D$, reflects whether observed spectra are explained in the Markov approximation or beyond the Markov

approximation. Markov approximation is valid for cases in which $\gamma_D > \Delta E$ or $\tau_c \equiv \frac{1}{\gamma_D} < \frac{1}{\Delta E} \equiv t$ is satisfied. That is, the bath correlation time is short compared with the time regime for observation. In this case, each phase of the off-diagonal elements in the reduced density matrix exponentially decays with a dephasing constant Γ. The dephasing constant can be expressed in terms of the Drude bath mode parameters (λ and γ_D) and temperature T as $\Gamma = 2\lambda k_B T/\gamma_D$ (see the Appendix). For $\gamma_D < \Delta E$, i.e., $\tau_c \equiv \frac{1}{\gamma_D} > \frac{1}{\Delta E} \equiv t$, the Markov approximation breaks down.

Consider a weak coupling case. Here $\lambda = 0.01$ eV, which satisfies the weak coupling condition $\lambda_D(= 0.01$ eV$)$ $< \Delta E_{b_2 b_1}(= 0.065$ eV$)$, was adopted. Figure 1(a) shows the time evolution of coherent ring currents $I_{b_1,b_2}(t)$ calculated with $\gamma_D = 0.50$ eV at $T = 298$ K. In Fig. 1(a), the quantum beats $I_{b_1,b_2}(t)$ in red color denote those calculated by the HEOM procedure. In the following discussions, the number of tiers was set to be tier $= 4$ and [N/N] PSD was carried out with $N = 3$; however, in Fig. 1(b) comparison of with and without Padé spectrum decomposition $N = 0$ and $N = 3$ is discussed. For comparison, the time-dependent ring current in the Markov approximation is drawn by the dotted line in red color. In the Markov approximation, $I_{b_1,b_2}(t)$ can be expressed as $I_{b_1,b_2}(t) \sim \exp[-\Gamma_{b_1 b_2} t]\sin(\omega_{b_2 b_1} t)$. Here, the dephasing constant has the form $\Gamma_{b_1 b_2} = 2\lambda_D k_B T/\gamma_D = 1.03 \times 10^{-3}$ eV in the Drude model. It can be seen in Fig. 1(a) that the time-dependent behaviors in $I_{b_1,b_2}(t)$ obtained by the HEOM procedure with $N = 3$ are almost same as those in the Markov approximation. This is because the time-dependent behaviors of the coherent ring currents in Fig. 1(a) correspond to the motional narrowing limit since the parameter $\gamma_D = 0.50$ eV satisfies $\gamma_D > \Delta E (=0.065$ eV$)$, which corresponds to bath correlation time $1/\gamma_D = 1.3$ fs, and, furthermore, the classical fluctuation-dissipation theorem with the first term in Eqs. (9a)–(9c) can be safely adopted.[26]

Figure 1(b) shows three types of $I_{b_1,b_2}(t)$ calculated at $T = 77$ K. Here, the same Drude parameters as those in Fig. 1(a) were adopted. This means that the Markov approximation is valid in the time-dependent behaviors. The line in green color is $I_{b_1,b_2}(t)$ calculated by the HEOM procedure with $N = 0$, i.e., without any consideration of Padé spectrum decomposition. The line in black color represents $I_{b_1,b_2}(t)$ is calculated by the HEOM procedure with taking into account [3/3] Padé spectrum decomposition. The dotted line in red color is $I_{b_1,b_2}(t)$ calculated with $\Gamma_{b1b2} = 2.66 \times 10^{-4}$ eV in the Markov approximation in the Drude model. It can be found from the results shown in Fig. 1(b) that temperature dependence in the HEOM procedure must be taken into account at low temperatures.

Figures 2(a) and 2(b) show $I_{b_1,b_2}(t)$ calculated with the Dude parameter set ($\lambda_D = 0.01$ eV and $\gamma_D = 0.01$ eV) at $T = 298$ K (77 K). The lines in black in Figs. 2(a) and 2(b) denote $I_{b_1,b_2}(t)$ obtained by the HEOM procedure. In Fig. 2, the condition of $\gamma_D = 0.01$ eV $< \Delta E (= 0.065$ eV$)$ is satisfied. The bath correlation time is $\hbar/\gamma_D = 66$ fs. Therefore, in Fig. 2, the time-dependent behaviors of $I_{b_1,b_2}(t)$ for $t < 66$ fs should basically reflect a non-Markov nature. The dotted lines in blue in Figs. 2(a) and 2(b) denote $I_{b_1,b_2}(t)$ in the static limit, which is the opposite limit of the Markov approximation. In the
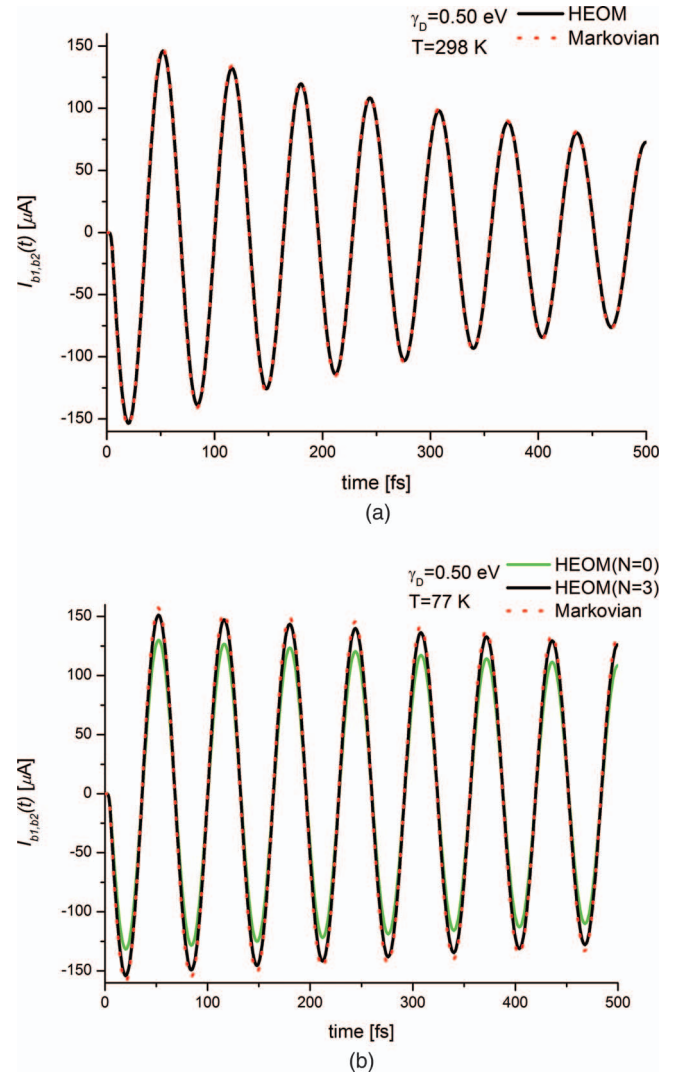

FIG. 1. (a) Time evolution of coherent ring currents $I_{b_1,b_2}(t)$ of (P)-2,2′-biphenol in a condensed phase in the Drude model at $T = 298$ K. The model calculations of $I_{b_1,b_2}(t)$ were carried out with the Drude parameter set ($\lambda = 0.01$ eV as the reorganization energy; $\gamma_D = 0.50$ eV as the damping parameter) under the weak coupling condition. The black line denotes $I_{b_1,b_2}(t)$ calculated by the hierarchical equation of motion (HEOM) procedure with tier $= 4$ for number of tiers and $N = 3$ for Padé spectrum decomposition (PSD). The dotted line in red color denotes $I_{b_1,b_2}(t)$ in the Markov approximation. Here, an exponential decay form was used for $I_{b_1,b_2}(t)$ with the dephasing constant $\Gamma_{b_1 b_2} = 1.03 \times 10^{-3}$ eV in the Drude model. (b) $I_{b_1,b_2}(t)$ at $T = 77$ K. The same Drude parameters as those in Fig. 1(a) were adopted. The line in green (black) color denotes $I_{b_1,b_2}(t)$ calculated by the HEOM procedure with $N = 0$ (3). The dotted line in red color denotes $I_{b_1,b_2}(t)$ calculated by the Markov approximation with dephasing constant $\Gamma_{b_1 b_2} = 2.66 \times 10^{-4}$ eV in the Drude model.

static limit, $I_{b_1,b_2}(t)$ can be approximately expressed in terms of a Gaussian form as $I_{b1b2}(t) \approx \exp[-i\omega_{b1b2} t - \frac{\Gamma_{b1b2}^{static} t^2}{2}]$ with $\Gamma_{b1b2}^{static} = 2\lambda k_B T$ (= 5.14×10^{-4} eV) for $T = 298$ K in the Drude model (See the Appendix). The time-dependent behavior is totally different from the other two lines, as expected. The Gaussian-type expression in $I_{b_1,b_2}(t)$ qualitatively reproduces the time-dependent behaviors for $t < 66$ fs in a short time regime that is around a half period of oscillation in quantum beats. However, it should be noted that the Gaussian-type expression fails to reproduce the time-dependent behaviors
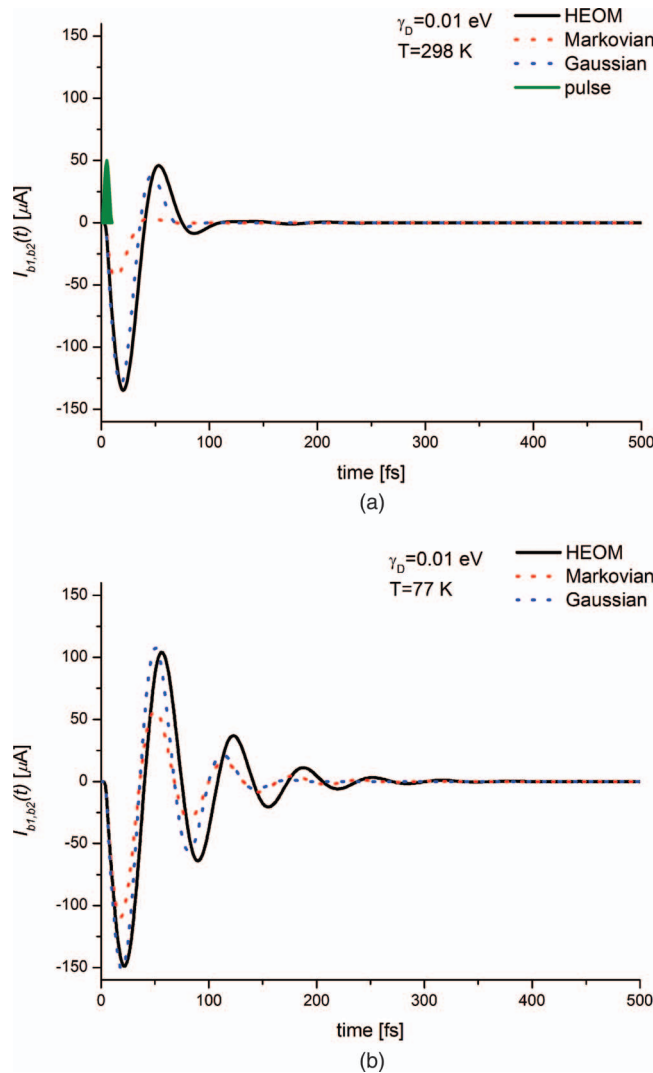
FIG. 2. (a) $I_{b_1,b_2}(t)$ of (*P*)-2,2′-biphenol in a condensed phase in the Drude model at $T = 298$ K. Drude parameters $\lambda = 0.01$ eV and $\gamma_D = 0.01$ eV were adopted under the weak coupling condition. The black line denotes $I_{b_1,b_2}(t)$ calculated by the HEOM procedure. The dotted line in blue color denotes $I_{b_1,b_2}(t)$ calculated in the static limit. Here a Gaussian form for $I_{b_1,b_2}(t)$ with dephasing constant $\Gamma_{b1b2}^{static} = 5.14 \times 10^{-4}$ eV^2 was used. The dotted line in red color denotes $I_{b_1,b_2}(t)$ in the Markov approximation with $\Gamma_{b_1b_2} = 5.14 \times 10^{-2}$ eV. The area in green color denotes the laser pulse shape, where the laser pulse duration $t_f - t_i = 10$fs. (b) $I_{b_1,b_2}(t)$ at $T = 77$ K. The same Drude parameters as those in Fig. 2(a) were adopted. The line in black color denotes $I_{b_1,b_2}(t)$ calculated by the HEOM procedure. The dotted line in blue color denotes $I_{b_1,b_2}(t)$ calculated with dephasing constant $\Gamma_{b1b2}^{static} = 1.33 \times 10^{-4}$ eV^2 in the static limit. The dotted line in red color denotes $I_{b_1,b_2}(t)$ calculated by the Markov approximation with dephasing constant $\Gamma_{b_1b_2} = 1.33 \times 10^{-2}$ eV.

FIG. 3. (a) $I_{b_1,b_2}(t)$ of (*P*)-2,2′-biphenol in a condensed phase in the Drude model at $T = 298$ K. Drude parameters $\lambda = 0.01$ eV and $\gamma_D = 0.03$ eV were adopted under the weak coupling condition. The black line denotes $I_{b_1,b_2}(t)$ calculated by the HEOM procedure. The dotted line in blue color denotes $I_{b_1,b_2}(t)$ calculated with $\Gamma_{b1b2}^{static} = 5.14 \times 10^{-4}$ eV in the static limit. The dotted line in red color denotes $I_{b_1,b_2}(t)$ in the Markov approximation with $\Gamma_{b_1b_2} = 1.71 \times 10^{-2}$ eV. (b) $I_{b_1,b_2}(t)$ at $T = 77$ K. The same Drude parameters as those in Fig. 3(a) were adopted. The line in black color denotes $I_{b_1,b_2}(t)$ calculated by the HEOM procedure. The dotted line in blue color denotes $I_{b_1,b_2}(t)$ calculated with dephasing constant $\Gamma_{b1b2}^{static} = 1.29 \times 10^{-4}$ eV^2 in the static limit. The dotted line in red color denotes $I_{b_1,b_2}(t)$ calculated by the Markov approximation with dephasing constant $\Gamma_{b_1b_2} = 4.28 \times 10^{-3}$ eV.

calculated by the HEOM procedure, which shows more than one cycle oscillation of quantum beats even at a high temperature of T = 298 K. For comparison, a dotted line in red denotes $I_{b_1,b_2}(t)$ calculated within the Markov approximation.

In Fig. 2(b), $I_{b_1,b_2}(t)$ calculated by the HEOM procedure and that calculated by the static limit are semi-quantitatively the same time-dependent behaviors at T = 77 K. Again, it can be seen that there is a deviation between the two lines for $I_{b_1,b_2}(t)$: the quantum beats in $I_{b_1,b_2}(t)$ calculated by the HEOM procedure are preserved in a much longer time regime near 300 fs, while those calculated in the static limit dissipate
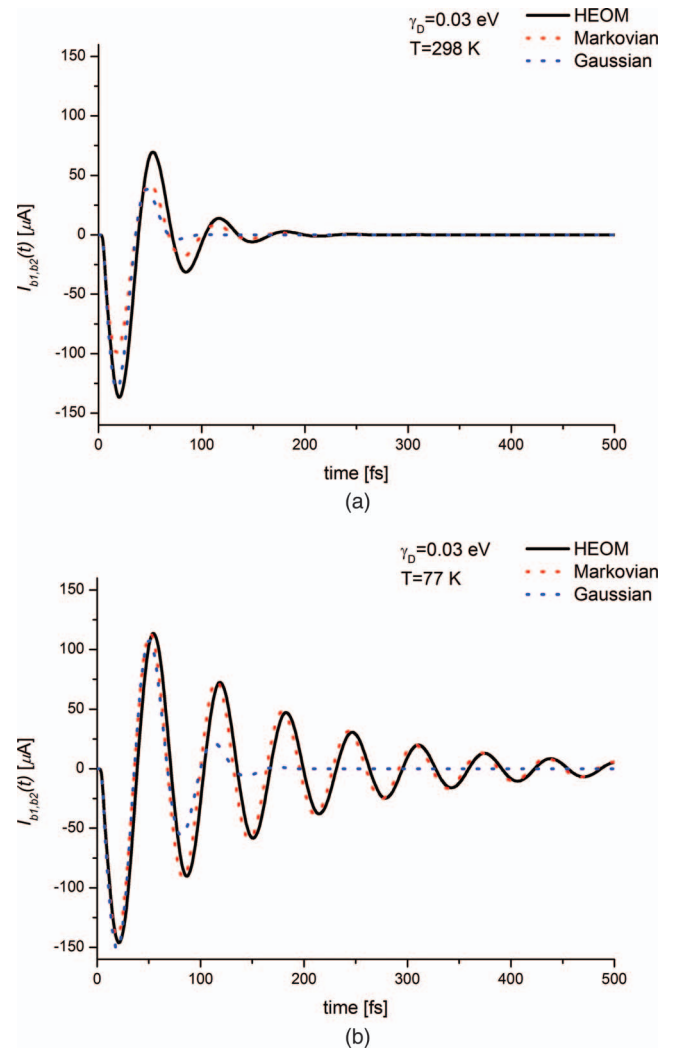
around at 150 fs. The existence of such a deviation indicates that the HEOM procedure is necessary to quantitatively explain the non-Markov response to coherent ring currents even in the static regime beyond Gaussian dephasing treatment.

Figure 3 shows time-dependent behaviors of $I_{b_1,b_2}(t)$ for the Drude parameter set ($\lambda = 0.01$ eV and $\gamma_D = 0.03$ eV) at $T = 298$ K (77 K). The difference in temperature dependence between the quantum beat signals in the static limit and those in the Markov approximation is notable. At $T = 77$ K, the signals in the Markov approximation semi-quantitatively reflect those in the HEOM even in the short time regime, while those calculated in the static limit reproduce only at the initial time regime within a half period of quantum beat oscillation. In this

paper, a semiclassical Drude model was adopted as the bath modes. At low temperatures, quantum behaviors in the bath modes may play an important role in the beat signal, and a model appropriate for bath modes at low temperatures should be treated beyond the semiclassical Drude model. There are several models for bath modes including harmonic oscillator model and Brownian oscillator model. The optimized HEOM theory has also been constructed for quantum dissipation in a bath environment with multiple Brownian oscillators.[25] It is applicable to dephasing effects in ultrafast coherent ring currents in low temperature cases to clarify the non-Markovian response at low temperatures.

Physically, non-Markovianity occurs whenever the system back-action on environment plays roles. However, the measure of non-Markovianity is not unique.[51,52] Recently Xu *et al.*[27] proposed the so-called *dynamical inhomogeneity parameter*, defined as

$$\alpha = \max\left\{ \alpha_{a,k} = \left| \frac{c_{a,k}}{2\gamma_{a,k}^2} \right| \right\} \quad a = 0, 1 \quad k = D, 1, \dots, N.$$
(14)

This dimensionless parameter depends only on the exponential expansion component of bath correlation function as in Eq. (7). We will see below it does serve as a convenient measure on the non-Markovianity of the system dynamics. Evidently, the bath is effective a white noise when $\alpha \ll 1$ (assuming also that the inverse of bath fluctuation timescale, γ_{max}, is larger than the system characteristic frequency). According to Eqs. (9a)–(9c), we have $\alpha_{a,D} = |\lambda_a f_{[N/N]}(-i\beta\gamma_{a,D})/\gamma_{a,D}|$ and $\alpha_{a,k} = |\eta_k J_a(-i\gamma_k)/\beta\gamma_k^2|(k = 1, \dots, N)$. We remark that for high temperature case $\alpha_{a,D}$ is much larger than other $\alpha_{a,k}(k = 1, \dots, N)$, while for low temperature case $\alpha_{a,D}$ and certain $\alpha_{a,k}(k = 1, \dots, N)$ become more comparative. Therefore, when temperature is lower, the contributions from $k = 1, \dots, N$ are often not negligible. In order to see the Markovinicity we considered the time-dependent behaviors of quantum beats at the initial time region $0 < t < 1/\Delta E$, with two parameters ΔE and γ_D. The evaluated values of a corresponding to Figs. 1(a), 2(a), and 3(a) (Figs. 1(b), 2(b), and 3(b)) are $\alpha = 0.01, 2.6$, and 0.3 ($\alpha = 0.01, 0.7$, and 0.2), respectively. It can be seen that Markovianity seems to be stronger at lower temperatures. We remark that parameter α to test Markovianity shows reasonable agreement with our numerical results for above cases. For $\alpha \ll 1$, as the cases of Figs. 1(a) and 1(b), the numerical results clearly indicate the Markovian dynamics; whereas for $\alpha > 1$ as in Fig. 2(a), a strong non-Markovianity is evident. In particular the cases with $\alpha \approx 1$ would reflect comparative Makovian and non-Markovian properties. The larger a value is the further away from Markovian; see, for example, Figs. 2(b), 3(a), and 3(b), with $\alpha = 0.7, 0.3$, and 0.2, respectively.

The above observations represent a quantitative explanation on Markovinicity, in terms of the dynamical inhomogeneity parameter α. The demonstrations are made through the comparison between the HEOM results and those from the Markovian theory. However, as discussed by Tanimura and Wolynes,[54] the appearance of damping in quantum beats caused by non-Markovian noise may be reproduced with an effective Markovian noise of weaker

coupling strength. This situation would also occur in the simulation of linear spectroscopy. Fortunately, multiple dimensional spectroscopy can provide an experimental means to "visualize" the non-Markovianity, for example, via the ratio of auto-correlation spectrum signal broadenings along the diagonal and anti-diagonal directions.[27] The same dynamical inhomogeneity parameter, α, of Eq. (14), works also for the non-Markovianity in nonlinear spectroscopic measurements.[27]

Recently, Dijkstra and Tanimura[55] showed that nonlinear optical response can also decipher the initial correlation induced non-Markovianity. To see whether the related type of non-Markovianity can be reflected in time-dependent coherent ring current experiments, we consider the nonlinear response of coherent ring currents $I_{b_1,b_2}(t)$ of (P)-2,2'-biphenol by applying a laser pulse with much longer pulse profile. The following laser pulse parameter set is used: $A(t) = F_0 g(t, t_i = 0, t_f = \frac{2\pi}{\omega_{b2b1}} = 64\,\text{fs})$ with $F_0 = 1.2\,\text{GV/m}$, for the same Drude dissipation case ($\lambda = 0.01$ eV, $\gamma_D = 0.01$ eV) in Figure 2(a), at T = 298 K. The results are shown in Figure 4. Compared with the results in Figure 2(a), in Figure 4 the deviation of $I_{b_1,b_2}(t)$ calculated by HEOM from that calculated by the Gaussian-type expression becomes much larger. The increase of non-Markovianity exhibited by the laser pulse with longer time profile indicates the non-Markovianity originates from the initial correlations between the two electronic states and the bath since the nonlinear interactions between π electrons and radiation fields increase for longer pulse case.

In the present treatment, (P)-2-2'-biphenols were assumed to be frozen in an embedded state in a solid, omitting molecular vibrations. It has already been recognized that intramolecular vibrations directly affect dephasing processes of ring currents through nonadiabatic couplings. In actual molecular systems, both intramolecular vibrations and intermolecular vibrations have significant effects on the ring
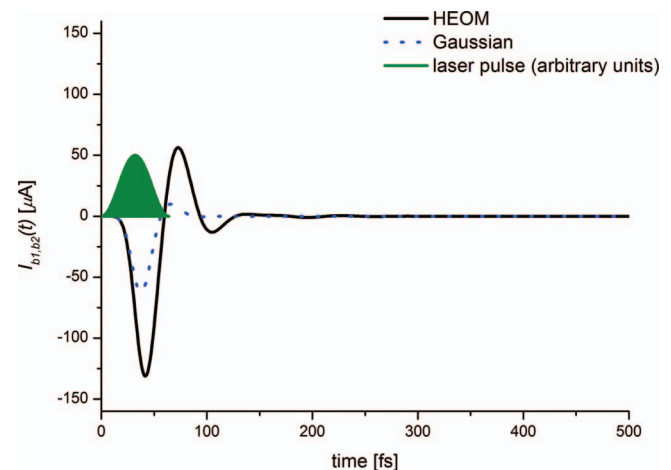

FIG. 4. $I_{b_1,b_2}(t)$ of (P)-2,2'-biphenol in a condensed phase in the Drude model at $T = 298$ K. The same Drude parameters as those in Fig. 2(a) were adopted. The black line denotes $I_{b_1,b_2}(t)$ calculated by the HEOM procedure. The dotted line in blue color denotes $I_{b_1,b_2}(t)$ calculated in the static limit. Here a Gaussian form for $I_{b_1,b_2}(t)$ with dephasing constant $\Gamma_{b1b2}^{static} = 5.14 \times 10^{-4}$ eV^2 was used. The area in green color denotes the laser pulse shape, where the laser pulse duration $t_f - t_i = 64$ fs.

currents of molecules.[56,57] It would be interesting to investigate the interplay between the two dephasing processes originating from intramolecular and intermolecular vibrations.

IV. CONCLUSION

In this paper, we examined the non-Markov response to femtosecond coherent ring currents in chiral aromatic molecules in a condensed phase. Our treatment was based on a hierarchical equation of motion (HEOM) procedure. A semiclassical Drude model was adopted for the heat baths. Simulations of the quantum beat signals $I_{b_1,b_2}(t)$ of (P)-2,2′-biphenol in a condensed phase were carried out in the weak molecule-heat bath coupling case. The important parameter of the Drude model, γ_D, dependence on the signals, was calculated, and non-Markov behaviors were clarified by comparing both $I(t)$ with those in the Markov approximation and those in the static limit. It was found that the beat signals calculated by the HEOM approach appear even in the time regime beyond the static limit because of the back actions of the bath modes to the current-generating molecules. This indicates that the non-Markov response has an important role in appearance of coherent ring currents in aromatic molecules in a condensed phase. This is a general phenomenon in ultrafast coherent dynamical processes of molecular systems in a condensed phase.

APPENDIX: DEPHASING CONSTANTS IN THE DRUDE MODEL

Let us derive an expression for the equation of motions of the reduced molecular density operator in the Markov approximation. In the classical Drude bath model, bath fluctuation effects are solely described from Eq. (9a) in terms of the bath correlation function,

$$C(t) = c_D \exp(-\gamma_D t), \tag{A1}$$

with $c_D = 2\lambda k_B T$.

The correlation function is equivalent to that in the Gaussian-Markovian process. The correlation function associated with two molecular states, a and b, has the form[49]

$$C_{ab}(t) = |v_{ab}|^2 \exp\left(-\frac{t}{\tau_c}\right). \tag{A2}$$

By comparison with the two expressions for the correlation function, the coupling matrix element has the form $v_{ab} = \sqrt{2\lambda k_B T}$. The correlation time τ_c is given as $\tau_c = 1/\gamma_D$. From the above treatment, one can obtain the expression for the density matrix element as

$$
\begin{aligned}
\rho_{ab}(t) &= \exp\left[-i\omega_{ab}t - \int_0^t dt_1 \int_0^{t_1} dt_2 C_{ab}(t_2)\right] \\
&= \exp\left[-i\omega_{ab}t - |v_{ab}|^2\tau_c^2\left\{\exp\left(-\frac{t}{\tau_c}\right) - 1 + \frac{t}{\tau_c}\right\}\right].
\end{aligned}
\tag{A3}
$$

Now, the time-dependent off-diagonal density matrix element in the Markov approximation can be expressed by taking $\frac{t}{\tau_c} \to \infty$ as

$$\rho_{ab}(t) \approx \exp\left[-i\omega_{ab}t - \Gamma_{ab}t\right]. \tag{A4}$$

Here Γ_{ab} is the dephasing constant in the Drude bath model, and is given as

$$\Gamma_{ab} \equiv |v_{ab}|^2 \tau_c = \frac{2\lambda k_B T}{\gamma_D}. \tag{A5}$$

In a similar way, the off-diagonal density matrix element in the static limit case is expressed by restricting expansion of the exponent in Eq. (A3) to an order of t^2 in a short time limit as

$$\rho_{ab}(t) \approx \exp\left[-i\omega_{ab}t - \frac{\Gamma_{ab}^{static} t^2}{2}\right]. \tag{A6}$$

Here

$$\Gamma_{ab}^{static} = |v_{ab}|^2 = 2\lambda k_B T. \tag{A7}$$

[1]C. M. Guédon, H. Valkenier, T. Markussen, K. S. Thygesen, J. C. Hummelen, and S. J. van der Molen, Nat. Nanotechnol. **7**, 305 (2012).
[2]V. Mujica, M. Kemp, and M. A. Ratner, J. Chem. Phys. **101**, 6849 (1994).
[3]L. Y. Hsu and H. Rabitz, Phys. Rev. Lett. **109**, 186801 (2012).
[4]A. Matos-Abiague and J. Berankdear, Phys. Rev. Lett. **94**, 166801 (2005).
[5]E. Räsänen, A. Castro, J. Werchnik, A. Rubio, and E. K. U. Gross, Phys. Rev. Lett. **98**, 157404 (2007).
[6]J. E. Anthony, Chem. Rev. **106**, 5028 (2006).
[7]Y. Fujimura and H. Sakai, *Electronic and Nuclear Dynamics in Molecular Systems* (World Scientific, Singapore, 2011), p. 117.
[8]I. Barth and J. Manz, Angew. Chem., Int. Ed. **45**, 2962 (2006).
[9]I. Barth, J. Manz, Y. Shigeta, and K. Yagi, J. Am. Chem. Soc. **128**, 7043 (2006).
[10]I. Barth and J. Manz, *Progress in Ultrafast Intense Laser Science VI* (Springer, 2010), p. 21.
[11]K. Nobusada and K. Yabana, Phys. Rev. A **75**, 032518 (2007).
[12]M. Kanno, H. Kono, and Y. Fujimura, Angew. Chem., Int. Ed. **45**, 7995 (2006).
[13]M. Kanno, K. Hoki, H. Kono, Y. Fujimura, J. Chem. Phys. **127**, 204314 (2007).
[14]M. Kanno, H. Kono, Y. Fujimura, S. H. Lin, Phys. Rev. Lett. **104**, 108302 (2010).
[15]M. Kanno, H. Kono, and Y. Fujimura, *Progress in Ultrafast Intense Laser Science VII* (Springer, 2011), p. 53.
[16]H. Mineo, M. Yamaki, Y. Teranish, M. Hayashi, S. H. Lin, and Y. Fujimura, J. Am. Chem. Soc. **134**, 14279 (2012).
[17]H. Mineo, S. H. Lin, and Y. Fujimura, J. Chem. Phys. **138**, 074304 (2013).
[18]J. Ding, J. Xu, J. Hu, R. X. Xu, and Y. J. Yan, J. Chem. Phys. **135**, 164107 (2011).
[19]Y. Tanimura and R. K. Kubo, J. Phys. Soc. Jpn. **58**, 101 (1989).
[20]Y. Tanimura, J. Phys. Soc. Jpn. **75**, 082001 (2006).
[21]A. Ishizaki and Y. Tanimura, J. Phys. Soc. Jpn. **74**, 3131 (2005).
[22]R. X. Xu, P. Cui, X. Q. Li, Y. Mo, and Y. J. Yan, J. Chem. Phys. **122**, 041103 (2005).
[23]R. X. Xu and Y. J. Yan, Phys. Rev. E **75**, 031107 (2007).
[24]Q. Shi, L. P. Chen, G. J. Nan, R. X. Xu, and Y. J. Yan, J. Chem. Phys. **130**, 084105 (2009).

[25] J. Hu, M. Luo, F. Jiang, R. X. Xu, and Y. J. Yan, J. Chem. Phys. **134**, 244106 (2011); J. Hu, R. X. Xu, and Y. J. Yan, *ibid.* **133**, 101106 (2010).

[26] J. J. Ding, R. X. Xu, and Y. J. Yan, J. Chem. Phys. **136**, 224103 (2012).

[27] J. Xu, H. D. Zhang, R. X. Xu, and Y. J. Yan, J. Chem. Phys. **138**, 024106 (2013).

[28] R. P. Feynman and F. L. Vernon, Jr., Ann. Phys. (N.Y.) **24**, 118 (1963).

[29] J. Shao, J. Chem. Phys. **120**, 5053 (2004).

[30] Y. Yan, F. Yang, Y. Liu, and J. Shao, Chem. Phys. Lett. **395**, 216 (2004).

[31] Y. Zhou, Y. Yan, and J. Shao, Europhys. Lett. **72**, 334 (2005).

[32] Q. Shi, L. P. Chen, G. J. Nan, R. X. Xu, and Y. J. Yan, J. Chem. Phys. **130**, 164518 (2009).

[33] R. X. Xu, B. L. Tian, J. Xu, Q. Shi, and Y. J. Yan, J. Chem. Phys. **131**, 214111 (2009).

[34] A. Ishizaki and Y. Tanimura, J. Chem. Phys. **125**, 084501 (2006).

[35] A. Ishizaki and Y. Tanimura, J. Phys. Chem. A **111**, 9269 (2007).

[36] L. P. Chen, R. H. Zheng, Q. Shi, and Y. J. Yan, J. Chem. Phys. **132**, 024505 (2010).

[37] B. L. Tian, J. J. Ding, R. X. Xu, and Y. J. Yan, J. Chem. Phys. **133**, 114112 (2010).

[38] X. Zheng, J. S. Jin, and Y. J. Yan, J. Chem. Phys. **129**, 184112 (2008).

[39] X. Zheng, J. S. Jin, and Y. J. Yan, New J. Phys. **10**, 093016 (2008).

[40] X. Zheng, J. S. Jin, S. Welack, M. Luo, and Y. J. Yan, J. Chem. Phys. **130**, 164708 (2009).

[41] A. Ishizaki and G. R. Fleming, J. Chem. Phys. **130**, 234110 (2009).

[42] L. P. Chen, R. H. Zheng, Y. Y. Jing, and Q. Shi, J. Chem. Phys. **134**, 194508 (2011).

[43] B. Hein, C. Kreisbeck, T. Kramer, and M. Rodríguez, New J. Phys. **14**, 023018 (2012).

[44] J. Zhu, S. Kais, P. Rebentrost, and A. Aspuru-Guzik, J. Phys. Chem. B **115**, 1531 (2011).

[45] C. Kreisbeck, T. Kramer, M. Rodríguez, and B. Hein, J. Chem. Theory Comput. **7**, 2166 (2011).

[46] J. Strümpfer and K. Schulten, J. Chem. Theory Comput. **8**, 2808 (2012).

[47] H. Lee, Y. C. Cheng, and G. R. Fleming, Science **316**, 1462 (2007).

[48] A. Ishizaki and G. R. Fleming, J. Phys. Chem. B **115**, 6227 (2011).

[49] J. S. Xu, C. F. Li, M. Gong, X. B. Zou, C. H. Shi, G. Chen, and G. C. Guo, Phys. Rev. Lett. **104**, 100502 (2010).

[50] B. Bellomo, R. Lo Franco, and G. Compagno, Phys. Rev. Lett. **99**, 160502 (2007).

[51] H. P. Breuer, E. M. Laine, and J. Piilo, Phys. Rev. Lett. **103**, 210401 (2009).

[52] A. Rivas, S. F. Huelga, and M. B. Plenio, Phys. Rev. Lett. **105**, 050403 (2010).

[53] M. J. Frisch, G. W. Trucks, H. B. Schlegel *et al.*, Gaussian 09, Revision E.01, Gaussian, Inc., Wallingford, CT, 2009.

[54] Y. Tanimura and P. G. Wolynes, J. Chem. Phys. **96**, 8485 (1992).

[55] A. G. Dijkstra and Y. Tanimura, Philos. Trans. R. Soc. London, Ser. A **370**, 3658 (2012).

[56] H. Mineo, M. Kanno, H. Kono, S. D. Chao, S. H. Lin, and Y. Fujimura, Chem. Phys. **392**, 136 (2012).

[57] Y. Fujimura, H. Kono, T. Nakajima, and S. H. Lin, J. Chem. Phys. **75**, 99 (1981).